Transl. Stroke Res. (2015) 6:39–49
DOI 10.1007/s12975-014-0358-6

ORIGINAL ARTICLE

# Longitudinal Assessment of Imatinib's Effect on the Blood–Brain Barrier After Ischemia/Reperfusion Injury with Permeability MRI

**Zamir Merali · Jackie Leung · D. Mikulis · F. Silver · Andrea Kassner**

Received: 30 April 2014 / Revised: 23 June 2014 / Accepted: 3 July 2014 / Published online: 23 August 2014


**Abstract** Acute ischemic stroke (AIS) often results in degeneration of the blood–brain barrier (BBB), which can lead to vasogenic edema and an increased risk of intracerebral hemorrhage. Imatinib is an agent that may be able to protect the BBB and reduce the risk of the harmful consequences of BBB degeneration. We sought to measure the effect of Imatinib on the BBB after experimental stroke longitudinally in vivo with permeability dynamic contrast-enhanced MRI. Ischemia/reperfusion injury was induced with a transient middle cerebral artery occlusion surgery. Rats were given Imatinib at 2 and 20 h after stroke onset. Post-assessment included neurologic functioning, MR imaging, Evans Blue extravasation, Western blot, and immunohistology assay. Imatinib protected the BBB by 24 h but failed to decrease BBB permeability at an earlier time-point. Imatinib also reduced infarct volume, edema, and improved neurologic functioning by 24 h. Rats treated with Imatinib also had a higher expression of the BBB structural protein Zona occludens-1 and a reduction in nuclear factor-kappa beta (NF-κβ) activation. Imatinib is a promising agent to protect the BBB after AIS, but its effect on the BBB may not become prominent until 24 h after the onset of ischemia. This finding may help elucidate Imatinib's role in the clinical management of AIS and influence future study designs.

**Keywords** Blood–brain barrier · Acute stroke · Brain ischemia · Brain edema · Focal ischemia · MRI

Z. Merali · J. Leung · A. Kassner
Department of Physiology and Experimental Medicine, Hospital for Sick Children, Toronto, ON, Canada

D. Mikulis
Division of Neuroradiology, Joint Department of Medical Imaging, Toronto Western Hospital, Toronto, ON, Canada

F. Silver
Division of Neurology, University Health Network, Toronto, ON, Canada

A. Kassner (✉)
Department of Medical Imaging, University of Toronto, Toronto, ON, Canada
e-mail: andrea.kassner@sickkids.ca

## Introduction

After acute ischemic stroke (AIS) the blood–brain barrier (BBB) can degenerate, leading to further complications. A particularly devastating outcome of this degeneration is hemorrhagic transformation (HT) [1, 2]. Early BBB degeneration after AIS is believed to be a precursor of HT [3]. Clinical studies using permeability MRI have shown a correlation between BBB permeability after AIS and the risk of eventual HT [4, 5]. However, in cases of ischemic stroke that do not progress to HT, degeneration of the BBB can still lead to vasogenic edema, which results in neuronal death and impaired neurobehavioral recovery [6, 7]. A further correlate of BBB degeneration after AIS is an increased extravasation of neutrophils into the central nervous system (CNS) tissue, which through the release of deleterious factors such as reactive oxygen species (ROS) can contribute to neuronal death and further degeneration of the BBB [8, 9]. The BBB degeneration after AIS can persist, due to a chronic down regulation of BBB structural proteins, particularly Zona occludens-1 (ZO-1) [10, 11]. Therefore, there is potential clinical utility in agents that can protect the BBB after AIS.

One such agent is the platelet-derived growth factor receptor (PDGFR) inhibitor, Imatinib [12–15]. Imatinib's effect on BBB permeability after AIS can be quantified with the ex vivo Evans blue assay. Such dye-based ex vivo assays, however, over-estimate permeability and have been criticized for inaccuracies due to the dye's tendency to bind reversibly to serum albumin [16]. A highly robust alternative is to assess BBB

permeability in vivo by analyzing the leakage of Gadolinium from vessel to brain tissue using dynamic contrast-enhanced (DCE) MRI [17]. This technique can be used to quantitatively assess how Imatinib affects the BBB longitudinally after experimental stroke and can be combined with in vivo assessment of brain edema, infarct size, and neurologic functioning. Such a longitudinal assessment may provide insight into the pathophysiologic evolution of AIS and the therapeutic window of Imatinib treatment.

In one study by Su et al. [13] Imatinib was shown to reduce extravasation of Evans blue dye in a permanent occlusion model, but this study was limited by the dye-based ex vivo method to assess the BBB. Moreover, by using a permanent occlusion model this study did not account for the substantial effect of reperfusion injury and the inflammatory response on the BBB [18, 19]. Experiments with a transient occlusion model, which more accurately model reperfusion injury and the inflammatory response, have not been done [20].

In the present study, we used the well-validated transient middle cerebral artery occlusion (tMCAo) model of AIS to assess how Imatinib affected the BBB. This study differed from the previous study by Su et al. by delaying the administration of Imatinib, utilizing a transient occlusion model, and utilizing a permeability MRI technique to quantify BBB permeability along with infarct size and edema in vivo at multiple time-points.

## Materials and Methods

### Animals

The Animal Care Committee at the Hospital for Sick Children approved all procedures for this study under the Canadian Council of Animal Care guidelines. Male Sprague–Dawley rats aged 59–67 days and 250–300 g in weight, were maintained in large cages under a 12-h light/dark cycle with temperature control (22 °C) and food/water available ad libitum.

### Experimental Design

The experimental timelines for the imaging and ex vivo experiments are shown in Fig. 1. For the imaging experiment, 25 rats were randomized via coin toss into control and treatment groups. Both groups underwent tMCAo surgery and the treatment group was given 100 mg/kg Imatinib mesylate (Novartis) via tail-vein injection at 2 h after stroke onset and an equivalent dose at 20 h to maintain the serum concentration. This dosage was chosen as it corresponds to the maximum indicated dose in humans [21]. An IV route of administration was chosen to mimic the clinical setting of AIS. Control rats were given equivalent volumes of saline at 2 and 20 h. In vivo tests were as follows: neurologic scoring at 0.5, 5, and 24 h to quantify neurologic deficit; MRI at 5 and 24 h to assess BBB permeability, infarct volume, and edema. Rats were sacrificed at 24 h with an intra-peritoneal Euthanyl injection and a subset underwent the Evans Blue assay to confirm BBB permeability.

An additional seven rats underwent tMCAo surgery and drug administration (three control and four treatment) but did not undergo MRI. In this set of rats stroke was confirmed with tetrazolium chloride (TTC) staining after sacrifice and brain tissue was collected for immunohistochemistry (IHC) to quantify neutrophil presence in the CNS and Western blotting to quantify nuclear factor-kappa beta (NF-κβ) activation and expression of ZO-1. Researchers were blinded to group allocation for all experiments and assessments.

### Middle Cerebral Artery Occlusion

Rats were anesthetized with isoflurane (3 % induction, 1–2 % maintenance). Focal ischemia was induced with the tMCAo model [22] with the following modifications: A commercially available silicone-coated suture measuring 0.3×5–6 mm (Doccol, Sharon, MA, USA) was used as this type of suture increases the reproducibility of stroke modeling [23]. The occlusion was maintained for 1 h before the suture was carefully retracted for reperfusion. Temperature and heart rate were measured continuously during the surgery. Rats were given 2 ml of fluids subcutaneously immediately after the surgery, and an additional 2 ml at 5 h after occlusion to reduce dehydration secondary to decreased ambulatory ability. Postoperative pain relief was provided with Temgesic (0.03 mg/kg) administered subcutaneously.

### Magnetic Resonance Imaging

MR imaging included T2 (TR/TE=4,800/72 ms) and T1 (T1FLASH, TR/TE=500/3 ms), diffusion-weighted imaging (DWI, with b=0.1000, TR/TE=1,000/33 ms), time-of-flight magnetic resonance angiography (MRA; 2DTOF, TR/TE=21.5/4.5 ms, slice=0.4 mm), and DCE imaging (discussed below). All of these examinations were performed on a 3 T system (Philips Achieva 3.0 T TX) using an eight-channel wrist coil. Prior to each imaging session a catheter was inserted into the tail-vein for injection of MR contrast media. BBB permeability was estimated with the DCE sequence, which was always performed after the structural data was acquired. DCE imaging consisted of a T1-weighted dynamic acquisition with the following parameters: TR/TE=6.3/2.2, FOV=100×85 $mm^2$, matrix=168×142, slice thickness=1 mm, volumes=36, time=4:20 min, slices=12 (entire infarct was covered). Gadolinium contrast agent was injected through the tail vein at a rate of 60 μl over 12 s beginning 21 s after the start of the DCE acquisition.

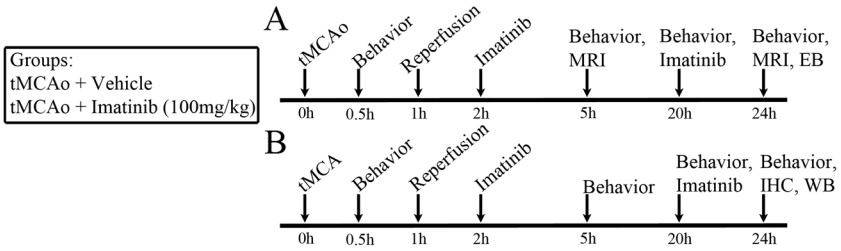


**Fig. 1** Experimental timelines for the imaging experiment (**a**) and ex vivo experiment (**b**). *tMCAo* transient middle cerebral artery occlusion, *Behavior* the modified Garcia neurologic test, *WB* Western blot, *EB* Evans Blue assay, *IHC* tissue extraction for histological preparation/immunohistochemistry

## Image Analysis

MRI data were analyzed to determine reperfusion status of the MCA, infarct volume, edema, and the permeability of the BBB.

MRA images were analyzed visually in OsiriX (v5.6 Pixmeo, Switzerland). The anterior–posterior maximum intensity projection was used and inadequate reperfusion was defined as an absent MCA signal within the infarcted hemisphere.

BBB permeability was estimated from the DCE data using in-house software (MR Analyst v2.1; University of Toronto, Canada) written in MATLAB v.7.11 (Mathworks, Natick, MA, USA). DCE images were co-registered to T2-weighted anatomical images and symmetric ROIs were manually defined to encompass the infarcted tissue and a corresponding region in the contralateral hemisphere. A third ROI was positioned within the sagittal sinus to determine the contrast agent concentration in the blood. As described in previous studies, voxel-by-voxel analysis of permeability was performed to generate permeability constant (KPS) maps over the infarcted regions and results are shown for representative animals from the control and treatment groups in Fig. 2a [4, 5, 24]. Briefly, a unidirectional two-compartment kinetic model was utilized to model the relationship between the blood concentration–time curve of the contrast agent and the mean tissue concentration of the contrast agent [25]. KPS was expressed as ml/100 mg/min. The KPS was then averaged over the infarcted tissue.

To determine infarct volume T2-weighted anatomical images were analyzed using OsiriX. Due to their higher resolution, the T2-weighted anatomical images offered better infarct visualization and quantification than DWI anatomical images. ROIs were manually defined on each slice encompassing the infarcted tissue to determine the cross-sectional area. Cross-sectional areas from all slices were summed to determine infarct volume.

To estimate edema, a previously validated protocol was used [26]. ROIs were manually defined on T2-weighted anatomical images on each slice encompassing the ipsilateral and contralateral hemispheres. The cross-sectional areas were summed across slices to give the total volume of the ipsilateral and contralateral hemispheres. The anatomic landmarks used to determine the midline boundary between hemispheres were the falx cerebri, aqueductus cerebri, third ventricle, fissure longitudinalis, and infundibulum. To quantify the extent of the edema in each rat, the average hemispheric volume was divided by the volume of the contralateral hemisphere.

## Evans Blue Extravasation

In a subset of the rats that underwent MRI evans blue extravasation into the CNS tissue was assessed as previously described [27]. Briefly, 200 μl of 4 % Evans Blue solution in saline was injected via the tail-vein 30 min prior to sacrifice. Then, 100 mg of brain tissue was extracted from the contralateral and ipsilateral hemispheres and homogenized with 0.5 ml of formalin. The tissue was pelleted via centrifugation and absorbance was measured in the supernatant at 610 nm to quantify Evans Blue extravasation against a set of standards. Levels of extravasated Evans Blue were expressed as ng of Evans Blue per mg of tissue.

## Neurologic Scoring

Neurologic scoring was completed with the modified Garcia test as has been previously described [28]. Briefly, we assessed spontaneous movement, symmetry of movement, symmetry of forelimbs, trunk sensation, and vibrissae sensation to generate a score out of 15.

## Histology

In the set of rats that did not undergo MRI, stroke was confirmed with the TTC stain. After sacrifice rat brains were extracted and quickly sectioned into 2-mm coronal slices over ice. A slice was incubated in TTC dye at 37 °C for 15 min. Rats with minimal or no infarcted tissue were excluded from further ex vivo testing.

IHC for myeloperoxidase (MPO) and H&E staining was performed by the staff at the Laboratory Medicine and Pathobiology at the Hospital for Sick Children to assess neutrophil levels. Tissue preparation methods were standardized in-house and equivalent to those used for clinical specimens. Briefly, a 2-mm slice of brain tissue was first dehydrated with

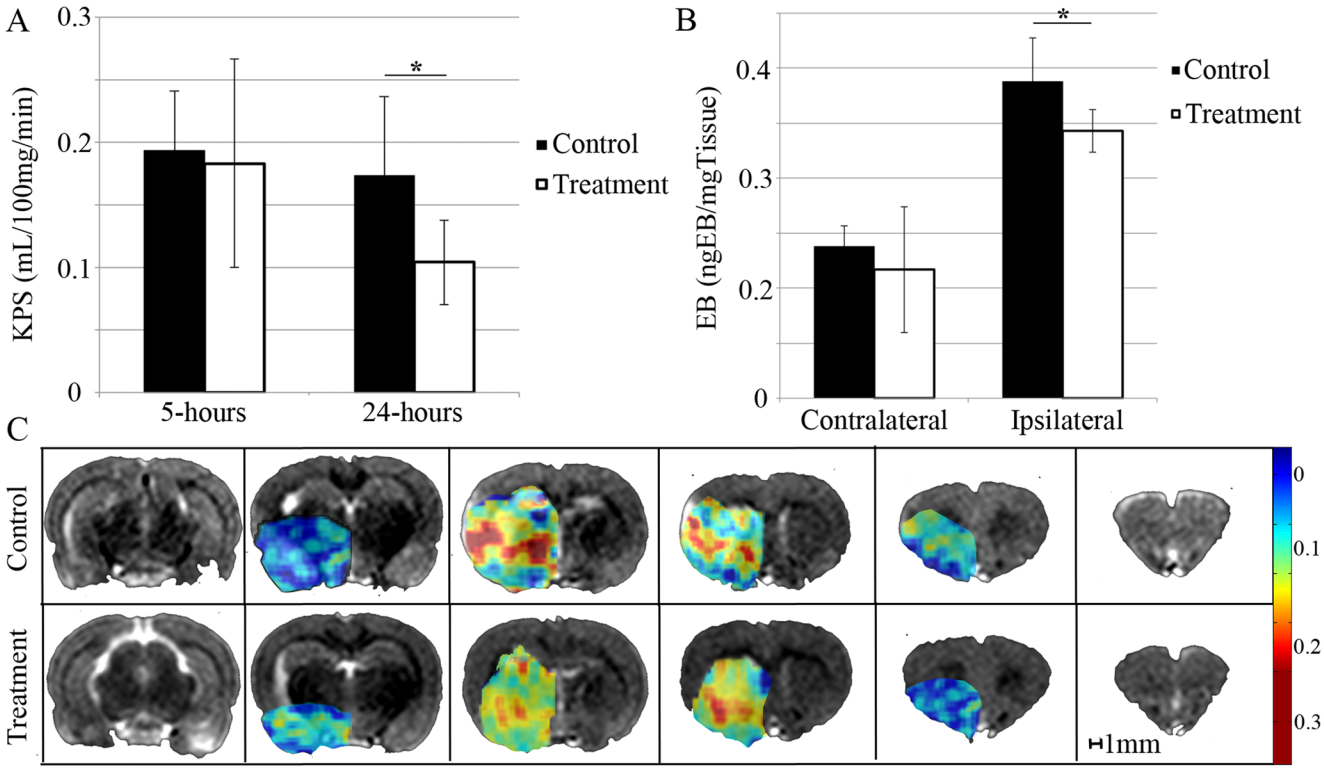


**Fig. 2** Evolution of blood–brain barrier (*BBB*) permeability after transient middle cerebral artery occlusion (*tMCAo*). **a** Permeability characteristics of the BBB as quantified by permeability magnetic resonance imaging at 5 and 24 h after tMCAo (group sizes, $n$=9). **b** Permeability characteristics of the BBB as quantified by the Evans Blue assay at 24 h after tMCAo (group sizes, $n$=4). **c** Representative permeability constant (KPS) maps from control and treatment groups showing BBB permeability over the infarcted areas at a single time-point in slices 2, 4, 6, 8, 10, and 12. *Error bars* represent standard deviation (*$p$<0.05, one-tailed)

a gradient of alcohol concentrations then embedded in paraffin wax using a tissue processor (Miles Tissue Tek; Sakura Finetek Inc., Torrance, CA, USA). Four 10-µm sections were prepared from formalin fixed tissue samples. IHC was also performed by the staff at the Laboratory Medicine and Pathobiology using in-house methods. Slides were scanned at 0.23-µm resolution (Zeiss Mirax Scanner). Levels of neutrophils were manually quantified within each hemisphere in ten random fields at 10× magnification per subject. Neutrophils were identified as cells having intact segmented nuclei and immunostaining around the periphery. Optical density measurements were also taken to quantify the MPO immunostaining within each hemisphere using the Image J software (NIH).

### Western Blots

Fifty mg of brain tissue was extracted from the contralateral and ipsilateral hemispheres, and whole-cell protein extracts were prepared. Primary antibodies used were: Phospho-NF-KappaB p65 (Ser536) (3033P, Cell Signaling) and ZO-1 (5406, Cell Signalling). Vinculin (5174P, Cell Signaling) was used as a loading control. Infrared conjugated secondary antibodies (LI-COR) were used and quantified using an Odyssey infrared imaging system.

### Statistics

Analyses were performed with the SPSS software v.18 (SPSS Inc., Chicago, IL, USA). Data was expressed as mean ± standard deviation of the mean and significance was determined with Student's $t$-tests (two-tailed) unless otherwise indicated. Neurologic scoring data was assessed with the Kruskal–Wallis one-way analysis of variance, as this data is ordinal and non-parametric. Sample sizes were calculated based on estimates of effect size from a previous relevant study [13].

## Results

Twenty-five rats underwent tMCAo and MR imaging. MRA revealed inadequate reperfusion in the MCA of two control rats and one treated rat. In addition, T1-weighted MR imaging at 5 h revealed intra-cerebral hemorrhage in one control rat and three treated rats. These rats were excluded from further analysis. Final group sizes for the imaging experiments were nine control rats and nine treated rats. Four rats from each group underwent Evans Blue staining ex vivo.

A further seven rats underwent tMCAo and TTC staining after sacrifice at 24 h. Final group sizes for the IHC and Western blotting experiments were four control and four treated rats (one control rat from the imaging experiment was used).

### Physiologic Parameters

Physiologic parameters are summarized in (Table 1). All of the rats undergoing tMCAo lost approximately 7 % to 13 % of their body weight over the 24-h recovery period. Weight loss did not differ between the treatment and control groups at any time-point ($p>0.05$). In all rats there was a transient increase in temperature by 0.9–1.2 °C after MCAO and temperatures returned to the normal range (36.1–36.9 °C) by 5 h after MCAO. There was no difference in temperatures between the control and treated groups at any time-point ($p>0.05$). All rats experienced a transient increase in heart rate by 72–126 beats/min (bpm) during the tMCAo surgery. By 24 h the heart rate in all rats had returned to the normal range (364±34 bpm). There was no difference in temperatures between the control and treated groups at any time-point ($p>0.05$).

### Imatinib Treatment Reduced Blood–Brain Barrier Permeability

Permeability MR imaging at 5 h revealed that KPS did not differ significantly between the treatment and control groups (Fig. 2a). By the end-point of 24 h, however, KPS was significantly ($p<0.05$, one-tailed) lower in the rats treated with Imatinib (0.10±0.03 ml/100 mg/min for the treatment group vs. 0.17±0.06 ml/100 mg/min for the control group). A one-tailed *t*-test was justified in this instance because of the previous indication of beneficial treatment effect [13].

As KPS is an in vivo estimate of BBB permeability we utilized the Evans Blue assay to confirm these results at the 24-h time-point (Fig. 2b). At 24 h, the rats treated with Imatinib had significantly ($p<0.05$, one-tailed) reduced extravasation of Evans Blue dye into the CNS tissue (0.49±0.03 ng/mg in the treatment group vs. 0.57±0.08 ng/mg in the control group, $n=4$). There was a moderate correlation ($R^2=0.432$, $p<0.05$) between DCE-MRI and Evans blue extravasation measurements.

The KPS was not homogenous across the infarcted areas (Fig. 2c). KPS was higher in the core of the infarct and lower in the periphery.

### Imatinib Treatment Reduces Infarct Volume and Edema

Control and treated rats subjected to a 1-h tMCAo surgery exhibited infarction in the right brain hemisphere at 5 and 24 h, as seen with hyper intensity on T2-weighted and diffusion-weighted MR imaging (Fig. 3a). In all animals, infarction was present throughout the basal ganglia at both the 5- and 24-h time-points. Specifically, the infarct consistently affected the internal capsule and the middle and posterior portions of the caudoputamen.

Figure 3b shows that in T2-weighted imaging at 5 h infarct volume did not differ significantly between the treatment and control groups (161.1±18.3 vs. 171.4±14.4 $mm^3$, respectively; $p=0.21$). By the end-point of 24 h, however, infarct volume was significantly ($p<0.05$) lower in the rats treated with Imatinib (222.7±60.7 $mm^3$ for the treatment group vs. 293.1±85.8 $mm^3$ for the control group). Cortical infarct volumes were 188.7±27.1 and 130.2±24.4 $mm^3$ for the control and treatment groups, respectively ($p<0.05$). Subcortical infarct volumes were 104.4±41.2 and 92.5±33.4 $mm^3$ for the control and treatment groups, respectively ($p=0.11$). Visually, we observed that Imatinib had reduced growth of the infarct into the cortical tissue.

(Fig. 3c) shows that edema at 24 h, as assessed by compression factor on T2-weighted images, was significantly ($p<0.05$) lower in the Imatinib treated rats (1.02±0.04 for the treatment group vs. 1.07±0.05 for the control group). Visually we observed that midline structures (falx cerebri, aqueductus cerebri, third ventricle, fissure longitudinalis, and infundibulum) were slightly displaced into the contralateral hemisphere in both control and Imatinib-treated rats.

### Imatinib Increases Neurologic Recovery After Ischemia/Reperfusion Injury

Marked neurologic impairment was observed in all rats at 0.5 and 5 h (Fig. 3d). In all rats, neurologic score had improved by 24 h but did not return to baseline value. Imatinib-treated rats showed significantly ($p<0.05$) improved neurologic score at 24 h (10.5±0.95 in the treatment group vs. 9±0.81 in the control group). No significant difference in neurologic score was seen between the treated and control groups before tMCAo or at 0.5 or 5 h after tMCAo ($p>0.05$).

### Imatinib Treatment Correlates with Reduced NF-κβ but Neutrophil Infiltration Is Unaffected

Because increased BBB permeability can correlate with neutrophil infiltration into the CNS, we measured the effect of Imatinib on neutrophil infiltration. Infiltrating neutrophils and MPO staining was seen in the ischemic regions of all rats that underwent tMCAo surgery at 24 h, as indicated in IHC slides (Fig. 4b). The contralateral hemispheres had low levels of neutrophils and a basal level of MPO staining. The infarcted hemispheres of Imatinib-treated rats showed a 18 % reduction in neutrophils but this measurement did not reach statistical significance ($p=0.14$, $n=4$) (Fig. 4a). The infiltrating neutrophils were not evenly distributed throughout the infarct but

**Table 1** Time course changes in physiologic parameters after middle cerebral artery occlusion in control and treatment groups

| | | 0 h | 0.5 h | 5 h | 24 h |
|---|---|---|---|---|---|
| Heart rate (BPM) | Control | 362±47 | 463±62 | 412±39 | 358±41 |
| | Treatment | 371±35 | 456±51 | 402±44 | 374±28 |
| Temperature (°C) | Control | 36.8±0.4 | 38.1±0.5 | 36.9±0.3 | 36.5±0.4 |
| | Treatment | 36.9±0.3 | 37.9±0.4 | 36.8±0.3 | 37.1±0.3 |
| Weight (g) | Control | 289±19 | 284±18 | 274±23 | 262±26 |
| | Treatment | 282±22 | 286±19 | 281±21 | 253±30 |

were concentrated around blood vessels and the borders of the infarct (Fig. 4b).

We measured the effect of Imatinib on NF-κβ activation after ischemia/reperfusion injury because activation of this complex can correlate with BBB permeability and Imatinib has been shown to affect NF-κβ activation in disease models other than AIS [29]. The infarcted hemispheres of all rats showed significantly increased levels of activated NF-κβ in comparison to the contralateral hemispheres ($p<0.0001$). The Imatinib-treated rats, however, had a 33 % decreased activation of NF-κβ in the infarcted hemisphere as seen with Western blot ($p<0.05$, $n=4$) (Fig. 5a).

### Imatinib Treatment Increases ZO-1 Expression

Since Imatinib had reduced BBB permeability by 24 h, we chose to measure the level of the junctional protein ZO-1 at this time-point as this protein can be assessed a marker of BBB structural integrity [10]. The infarcted hemispheres of all rats showed significantly reduced levels of ZO-1 in comparison to the contralateral hemispheres ($p<0.01$). The Imatinib-treated rats, however, had a 35 % increased expression of ZO-1 in the infarcted hemisphere as seen with Western blot ($p<0.05$, $n=4$) (Fig. 5b).

## Discussion

The onset of cerebral ischemia triggers a complex set of responses, which can lead to BBB degeneration, and HT [2]. Therapeutic intervention after stroke has the goal of interrupting these responses so as to reduce the harmful effects of cerebral ischemia. In the present study, we used permeability MRI to demonstrate that Imatinib protected the BBB at 24 h but not at an earlier time-point of 5 h. Although Imatinib

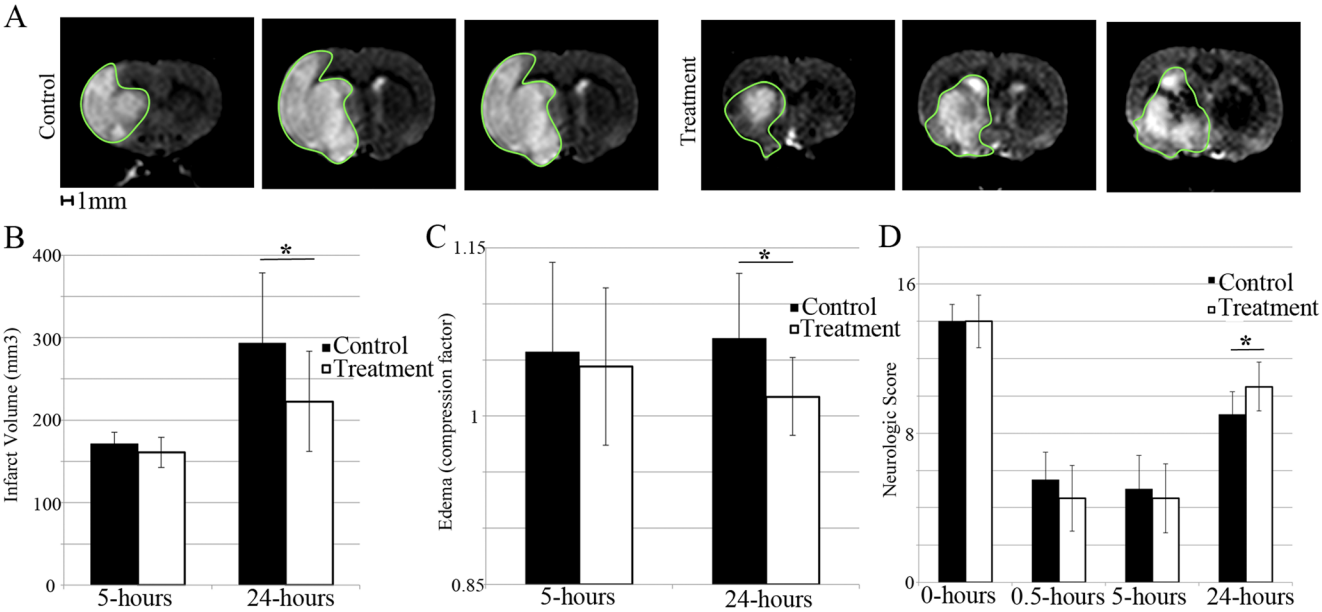


**Fig. 3** Evolution of infarct volume, edema, and neurologic functioning after transient middle cerebral artery occlusion (tMCAo). **a** Representative T2-weighted images from the control and treatment groups at 24 h showing infarcted tissue encircled by an ROI for lesion volume analysis. **b** Infarct volumes as quantified by analysis of T2-weighted magnetic resonance imaging (*MRI*) at 5 and 24 h after tMCAo (group sizes, $n=9$). Edema as quantified by analysis of T2-weighted MRI at 24-h (group sizes, $n=9$). **c** Neurologic score on the modified Garcia test at four time-points: before tMCAo, 0.5 h after tMCAo, 5 h after tMCAo, and 24 h after tMCAo (group sizes, $n=9$). *Error bars* represent standard deviation (*$p<0.05$)

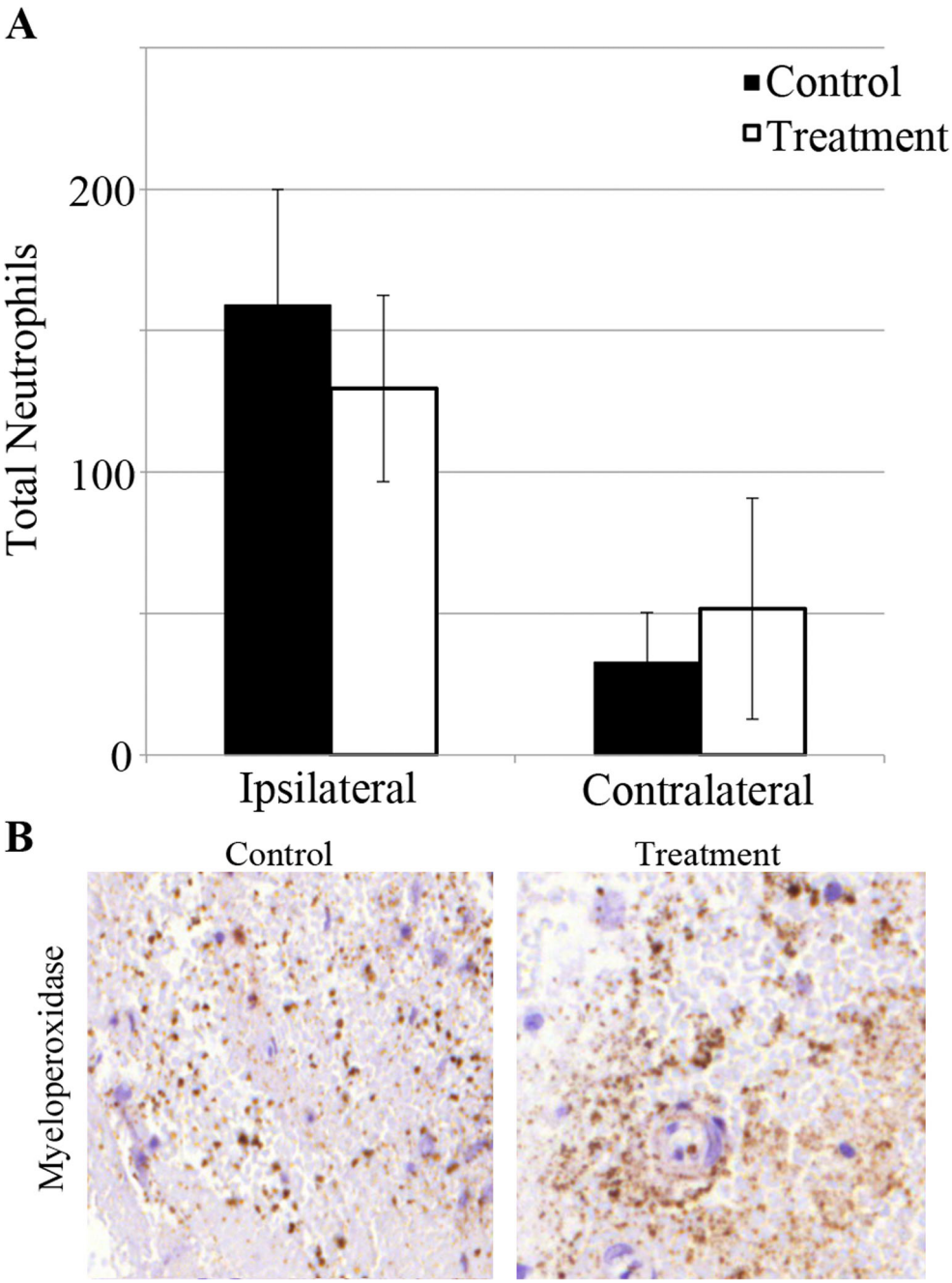


**Fig. 4** Immunohistochemistry with an H&E counter-stain was used to visualize neutrophil presence in the CNS by staining for myeloperoxidase in slices 2 mm rostral of bregma. **a** Quantification of staining intensity in ipsilateral and contralateral hemispheres (group sizes, $n$=4). **b** Representative micrographs of myeloperoxidase staining at 24 h. Error bars represent standard deviation ($p$= 0.14)

presents a valuable strategy to mitigate the risks of BBB degeneration after AIS, its efficacy may be limited immediately after an ischemic event.

## Imatinib Treatment Reduced BBB Permeability and Increased Levels of ZO-1

The change in KPS and Evans Blue extravasation both demonstrated that Imatinib had resulted in reduced BBB permeability by 24 h. However, BBB permeability was not reduced at the earlier time-point of 5 h. This suggested that Imatinib's effect on the BBB varied over the first 24 h after ischemia/reperfusion injury. Our results indicated that Imatinib might not reduce the risks associated with increased BBB permeability such as HT and vasogenic edema immediately after AIS. But by 24 h Imatinib may begin to mitigate these risks, because this is when the BBB protecting effect of Imatinib became prominent. The risk of HT is known to be

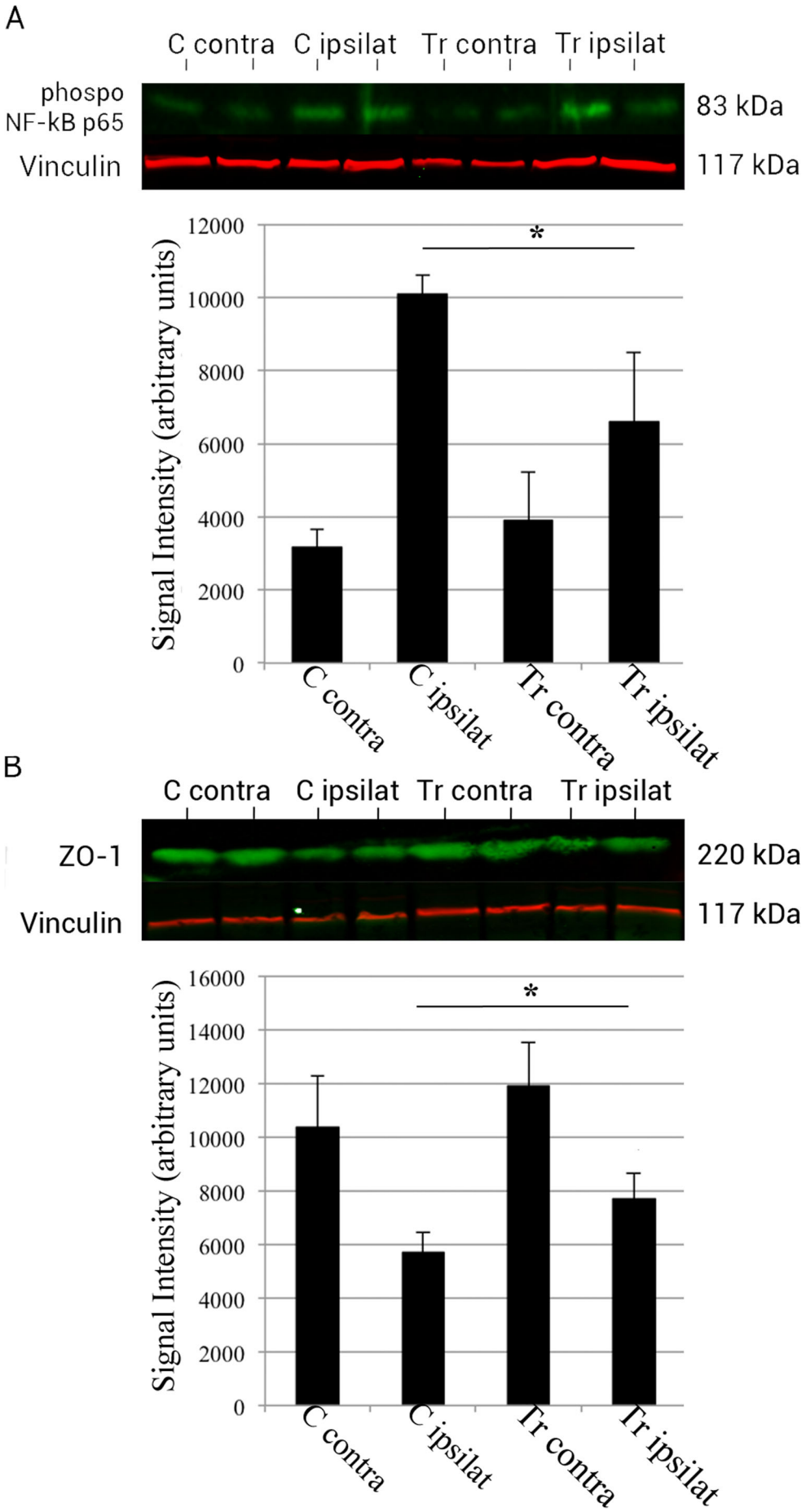
A
C contra
C ipsilat
Tr contra
Tr ipsilat
phospo NF-kB p65
Vinculin
83 kDa
117 kDa
Signal Intensity (arbitrary units)
12000
10000
8000
6000
4000
2000
0
*
C contra
C ipsilat
Tr contra
Tr ipsilat
B
C contra
C ipsilat
Tr contra
Tr ipsilat
ZO-1
Vinculin
220 kDa
117 kDa
Signal Intensity (arbitrary units)
16000
14000
12000
10000
8000
6000
4000
2000
0
*
C contra
C ipsilat
Tr contra
Tr ipsilat

◀ **Fig. 5** Levels of **a** phospho NF-κβ p65 and **b** ZO-1 expression (*green*) in the ipsilateral and contralateral hemispheres of control and Imatinib-treated rats. *C contra* Control contralateral hemisphere, *C ipsilat* Control ipsilateral hemisphere, *Tr contra* Treatment contralateral hemisphere, *Tr ipsilat* Treatment ipsilateral hemisphere. Expressions are normalized to vinculin expression (*red*) (group sizes, $n=4$). *Error bars* represent standard deviation (*$p<0.05$).

high at both 5 and 24 h after AIS, but it is not well understood precisely how this risk evolves with time. In addition, our results suggest that it may be possible to administer Imatinib at a later time-point than 2 h and still achieve protection of the BBB by 24 h.

Zona occludins-1 is a vital BBB structural protein involved in both occludin and tight-junction formation. Zona occludins-1 has been shown to be particularly abundant in the peripheral tight junctions of the BBB and can be measured alone as a marker of tight junction integrity after ischemia reperfusion injury [10, 11]. Previous studies have shown that ischemia/reperfusion injury caused a decreased expression of the ZO-1 tight-junction protein [11, 30]. Our results confirmed this finding, but also showed that Imatinib had caused an increase in ZO-1 expression by 24 h. Taken together, these results suggested that Imatinib might be able to protect the BBB and increase tight junction integrity through a mechanism involving increased ZO-1 levels. Future studies may also examine the effect of Imatinib on other BBB structural proteins such as the occludins and claudin-5.

## Imatinib Treatment Increases Tissue Preservation and Improves Neurologic Functioning

We observed that infarct volumes grew over the first 24 h after the onset of cerebral ischemia. This was in line with previous studies, which have shown that over the first 24 h, infarct volume grows to >80 % of the size achieved by 72 h [31]. At 24 h, we observed that Imatinib had reduced infarct volumes by 24 % compared to the control group. This strengthened the results of a previous study, which demonstrated that 200 mg/kg of Imatinib reduced infarct volume by 34 % when given 1 h after stroke onset in a permanent occlusion model [13]. Our study differed from this previous study as we used a transient occlusion model and first gave Imatinib at a later time-point (2 h) and at a lower dose (100 mg/kg). Structural MR imaging showed that, while the MCA territory was consistently infarcted in both control and treated rats, Imatinib had reduced the infarct growth beyond the MCA vascular territory (Fig. 2a).

Neurologic deficit after stroke is often the result of both neuronal death and increased intra-cranial pressure due to edema [32]. In support of this, we observed that an improvement in neurologic functioning at 24 h in the Imatinib-treated rats was accompanied by a reduction in infarct volume and edema.

## Imatinib Treatment Reduces NF-κβ Activation but Neutrophil Infiltration Is Unaffected

At the level of transcriptional regulation an important mechanism of immune activation and subsequent BBB degeneration is the NF-κβ. The activation of NF-κβ is seen in a variety of CNS disease models including transient focal ischemia, global ischemia, traumatic brain injury, and intra-cerebral hemorrhage [33, 34]. NF-κβ activation after transient focal ischemia can lead to increased inflammatory cytokine release, which may promote BBB degeneration through a variety of mechanisms [35]. Evidence for this comes from studies demonstrating that NF-κβ inhibition results in increased neuronal survival and a reduction of harmful inflammatory responses [36]. Interestingly, however, complete NF-κβ inactivation has been shown to lead to a reduction in anti-apoptotic genes and increased cell death after tMCAo in rats [37]. Complete inactivation of NF-κβ seems to be neurotoxic, while partial NF-κβ inhibition can interfere with diapedesis of inflammatory leukocytes into the CNS and seems to be neuroprotective. We evaluated NF-κβ activation and found this to be reduced but not eliminated with Imatinib treatment. Imatinib has been shown to cause a reduction in NF-κβ activation in conditions other than AIS [29]. This may be mediated through inhibition of the PI3K/AKT pathway although further work is needed to investigate this mechanism [38].

Increased BBB permeability can often correlate with neutrophil infiltration. Studies in rodent models show that neutrophils first appear in the CNS tissue at 2 h after vessel reperfusion and peak at 24–48 h [39]. This resembles the inflammatory response seen in human stroke [40]. Permanent models of focal ischemia do not show significant neutrophil infiltration. Activated neutrophils in the CNS tissue release a variety of deleterious compounds, including inflammatory cytokines, ROS, and activators of arachadonic acid cascades [41]. In the tMCAo model, neutrophil levels in the CNS correlate with infarct size, and suppression of neutrophil activity is neuroprotective, indicating that activated neutrophils in the CNS are partially responsible for cell death in the delayed phase [39]. In addition, many CNS neutrophils express matrix metalloproteinase 9 (MMP-9), which is known to contribute to BBB degeneration and HT after ischemic stroke [8]. Imatinib resulted in a reduction in CNS neutrophils at 24 h, but this comparison did not achieve statistical significance. Previous studies have shown that neutrophil infiltration is a major cause of BBB permeability after AIS. Our findings indicated that Imatinib was able to protect the BBB in the absence of a significant reduction in neutrophil infiltration. This finding is similar to a previous study on rodent spinal cord injury, which showed that Imatinib protected the spinal BBB but did not affect neutrophil infiltration into the spinal cord [12].

In conclusion, we have utilized the non-invasive permeability MRI technique to demonstrate that Imatinib's protective effect on the BBB is present by 24 h after occlusion but not at the earlier time-point of 5 h. As a result, Imatinib's beneficial effect may be limited immediately after AIS. Nonetheless, Imatinib is a common and relatively cost-effective therapeutic that shows promise to protect the BBB and reduce the risk of HT and vasogenic edema in the acute stage of AIS. Before this can occur, there is a need for additional supporting evidence and optimization. Future studies may establish a dose response and examine the effect of combined thrombolytic and Imatinib therapy.

**Acknowledgements** This work was supported by the Canada research chair program, Heart and Stroke Foundation of Canada, and Comprehensive research experience for medical students (CREMS).

**Conflict of interest** Zamir Merali, Jackie Leung, David Mikulis, Frank Silver, and Andrea Kassner declare that they have no conflict of interest. All institutional and national guidelines for the care and use of laboratory animals were followed.

## Reference

1. The NINDS t-PA Stroke Study Group. Intracerebral hemorrhage after intravenous t-PA therapy for ischemic stroke. Stroke. 1997;28(11):2109–18.
2. Donnan GA, Fisher M, Macleod M, Davis SM. Stroke. Lancet. 2008;371(9624):1612–23.
3. Xing C, Hayakawa K, Lok J, Arai K, Lo EH. Injury and repair in the neurovascular unit. Neurol Res. 2012;34(4):325–30.
4. Kassner A, Roberts T, Taylor K, Silver F, Mikulis D. Prediction of hemorrhage in acute ischemic stroke using permeability MR imaging. Am J Neuroradiol. 2005;26(9):2213–7.
5. Kassner A, Thornhill R. Measuring the integrity of the human blood–brain barrier using magnetic resonance imaging. Methods Mol Biol. 2011;686:229–45.
6. Armstead WM, Nassar T, Akkawi S, Smith DH, Xiao-Han C, Cines DB, et al. Neutralizing the neurotoxic effects of exogenous and endogenous tPA. Nat Neurosci. 2006;9(9):1150–5.
7. Sandoval KE, Witt KA. Blood–brain barrier tight junction permeability and ischemic stroke. Neurobiol Dis. 2008;32(2):200–19.
8. Rosell A, Cuadrado E, Ortega-Aznar A, Hernandez-Guillamon M, Lo EH, Montaner J. MMP-9-positive neutrophil infiltration is associated to blood–brain barrier breakdown and basal lamina type IV collagen degradation during hemorrhagic transformation after human ischemic stroke. Stroke. 2008;39(4):1121–6.
9. Paciaroni M, Agnelli G, Corea F, Ageno W, Alberti A, Lanari A, et al. Early hemorrhagic transformation of brain infarction: rate, predictive factors, and influence on clinical outcome: results of a prospective multicenter study. Stroke. 2008;39(8):2249–56.
10. Abbruscato TJ, Lopez SP, Mark KS, Hawkins BT, Davis TP. Nicotine and cotinine modulate cerebral microvascular permeability and protein expression of ZO-1 through nicotinic acetylcholine receptors expressed on brain endothelial cells. J Pharm Sci. 2002;91(12):2525–38.
11. Jiao H, Wang Z, Liu Y, Wang P, Xue Y. Specific role of tight junction proteins claudin-5, occludin, and ZO-1 of the blood–brain barrier in a focal cerebral ischemic insult. J Mol Neurosci. 2011;44(2):130—9. Jun 2011.
12. Abrams MB, Nilsson I, Lewandowski SA, Kjell J, Codeluppi S, Olson L, et al. Imatinib enhances functional outcome after spinal cord injury. PLoS One. 2012;7(6):e38760.
13. Su E, Fredriksson L, Geyer M, Folestad E, Cale J, Andrae J, et al. Activation of PDGF-CC by tissue plasminogen activator impairs blood–brain barrier integrity during ischemic stroke. Nat Med. 2008;14:731.
14. Ma Q, Huang B, Khatibi N, Rolland 2nd W, Suzuki H, Zhang JH, et al. PDGFR-alpha inhibition preserves blood–brain barrier after intracerebral hemorrhage. Ann Neurol. 2011;70(6):920–31.
15. Adzemovic MZ, Zeitelhofer M, Eriksson U, Olsson T, Nilsson I. Imatinib ameliorates neuroinflammation in a rat model of multiple sclerosis by enhancing blood–brain barrier integrity and by modulating the peripheral immune response. PLoS One. 2013;8(2):e56586.
16. Deli MA, Ábrahám CS, Kataoka Y, Niwa M. Permeability studies on in vitro blood–brain barrier models: physiology, pathology, and pharmacology. Cell Mol Neurobiol. 2005;25(1):59–127.
17. Hoffmann A, Bredno J, Wendland MF, Derugin N, Hom J, Schuster T, et al. Validation of in vivo magnetic resonance imaging blood–brain barrier permeability measurements by comparison with gold standard histology. Stroke. 2011;42(7):2054–60.
18. Durukan A, Tatlisumak T. Acute ischemic stroke: Overview of major experimental rodent models, pathophysiology, and therapy of focal cerebral ischemia. Pharmacol, Biochem Behav. 2007;87(1):179–97.
19. Liu S, Zhen G, Meloni BP, Campbell K, Winn HR. Rodent stroke model guidelines for preclinical stroke trials (1st edition). J Exp Stroke Transl Med. 2009;2(2):2–27.
20. Kriz J. Inflammation in ischemic brain injury: timing is important. Crit Rev Neurobiol. 2006;18(1–2):145–57.
21. Larson RA, Druker BJ, Guilhot F, O'Brien SG, Riviere GJ, Krahnke T, et al. Imatinib pharmacokinetics and its correlation with response and safety in chronic-phase chronic myeloid leukemia: a subanalysis of the IRIS study. Blood. 2008;111(8):4022–8.
22. Uluç K, Miranpuri A, Kujoth GC, Aktüre E, Başkaya MK. Focal cerebral ischemia model by endovascular suture occlusion of the middle cerebral artery in the rat. J Vis Exp. 2011;05((48):e1978.
23. Takano K, Tatlisumak T, Bergmann AG, Gibson III DG, Fisher M. Reproducibility and reliability of middle cerebral artery occlusion using a silicone-coated suture (Koizumi) in rats. J Neurol Sci. 1997;153(1):8–11.
24. Vidarsson L, Thornhill RE, Liu F, Mikulis DJ, Kassner A. Quantitative permeability magnetic resonance imaging in acute ischemic stroke: how long do we need to scan? Magn Reson Imaging. 2009;27(9):1216–22.
25. Patlak CS, Blasberg RG, Fenstermacher JD. Graphical evaluation of blood-to-brain transfer constants from multiple-time uptake data. J Cereb Blood Flow Metab. 1983;3(1):1–7.
26. Gerriets T, Stolz E, Walberer M, Müller C, Kluge A, Bachmann A, et al. Noninvasive quantification of brain edema and the space-occupying effect in rat stroke models using magnetic resonance imaging. Stroke. 2004;35(2):566–71.
27. Radu M, Chernoff J. An in vivo assay to test blood vessel permeability. J Vis Exp. 2013;73:e50062.
28. Garcia JH, Wagner S, Liu K, Hu X. Neurological deficit and extent of neuronal necrosis attributable to middle cerebral artery occlusion in rats: statistical validation. Stroke. 1995;26(4):627–35.
29. Ciarcia R, Vitiello MT, Galdiero M, Pacilio C, Iovane V, d'Angelo D, et al. Imatinib treatment inhibit IL-6, IL-8, NF-KB and AP-1 production and modulate intracellular calcium in CML patients. J Cell Physiol. 2012;227(6):2798–803.
30. Watson PM, Anderson JM, Vanltallie CM, Doctrow SR. The tight-junction-specific protein ZO-l is a component of the human and rat blood–brain barriers. Neurosci Lett. 1991;129(1).

31. Neumann-Haefelin T, Kastrup A, de Crespigny A, Yenari MA, Ringer T, Sun GH, et al. Serial MRI after transient focal cerebral ischemia in rats: dynamics of tissue injury, blood–brain barrier damage, and edema formation. Stroke. 2000;31(8):1965–73.
32. Xi G, Keep RF, Hua Y, Xiang J, Hoff JT. Attenuation of thrombin-induced brain edema by cerebral thrombin preconditioning. Stroke. 1999;30(6):1247–55.
33. Berti R, Williams AJ, Moffett JR, Hale SL, Velarde LC, Elliott PJ, et al. Quantitative real-time RT-PCR analysis of inflammatory gene expression associated with ischemia–reperfusion brain injury. J Cereb Blood Flow Metab. 2002;22(9):1068–79.
34. Nurmi A, Lindsberg PJ, Koistinaho M, Zhang W, Juettler E, Karjalainen-Lindsberg ML, et al. Nuclear factor-kappaB contributes to infarction after permanent focal ischemia. Stroke. 2004;35(4):987–91.
35. Carroll JE, Hess DC, Howard EF, Hill WD. Is nuclear factor-kappaB a good treatment target in brain ischemia/reperfusion injury? Neuroreport. 2000;11(9):R1–4.
36. Zhang L, Zhang ZG, Zhang RL, Lu M, Adams J, Elliott PJ, et al. Postischemic (6-Hour) treatment with recombinant human tissue plasminogen activator and proteasome inhibitor PS-519 reduces infarction in a rat model of embolic focal cerebral ischemia. Stroke. 2001;32(12):2926–31.
37. Hill WD, Hess DC, Carroll JE, Wakade CG, Howard EF, Chen Q, et al. The NF-kappaB inhibitor diethyldithiocarbamate (DDTC) increases brain cell death in a transient middle cerebral artery occlusion model of ischemia. Brain Res Bull. 2001;55(3):375–86.
38. Kim E, Matsuse M, Saenko V, Suzuki K, Ohtsuru A, Mitsutake N, et al. Imatinib enhances docetaxel-induced apoptosis through inhibition of nuclear factor-kappaB activation in anaplastic thyroid carcinoma cells. Thyroid. 2012;22(7):717–24.
39. Schofield ZV, Woodruff TM, Halai R, Wu MC, Cooper MA. Neutrophils — a key component of ischemia reperfusion injury. Shock. 2013 Oct 1.
40. Barone FC, Feuerstein GZ. Inflammatory mediators and stroke: new opportunities for novel therapeutics. J Cereb Blood Flow Metab. 1999;19(8):819–34.
41. Stanimirovic D, Satoh K. Inflammatory mediators of cerebral endothelium: a role in ischemic brain inflammation. Brain Pathol. 2000;10(1):113–26.